Functionalized polyester-based materials as UV curable adhesives

T. Cernadas, M. Santos, F.A.M.M. Gonçalves, P. Alves, T.R. Correia, I.J. Correia, P. Ferreira

PII: S0014-3057(19)31320-5
DOI: https://doi.org/10.1016/j.eurpolymj.2019.08.023
Reference: EPJ 9196

To appear in: *European Polymer Journal*

Received Date: 28 June 2019
Revised Date: 17 August 2019
Accepted Date: 19 August 2019

Please cite this article as: Cernadas, T., Santos, M., Gonçalves, F.A.M.M., Alves, P., Correia, T.R., Correia, I.J., Ferreira, P., Functionalized polyester-based materials as UV curable adhesives, *European Polymer Journal* (2019), doi: https://doi.org/10.1016/j.eurpolymj.2019.08.023

Functionalized polyester-based materials as UV curable adhesives

T. Cernadas[a], M. Santos[a], F. A. M. M. Gonçalves[a], P. Alves[a], T. R. Correia[b], I. J. Correia[a,b], P. Ferreira[a,*]

[a] CIEPQPF, Department of Chemical Engineering, University of Coimbra, P-3030 790 Coimbra, Portugal

[b] CICS-UBI, Health Sciences Research Center, University of Beira Interior, P-6200 506 Covilhã, Portugal

[*]Corresponding author: P. Ferreira, CIEPQPF, Department of Chemical Engineering, University of Coimbra, P-3030 790 Coimbra, Portugal

E-mail address: pferreira@eq.uc.pt

ABSTRACT

UV curable adhesives offer major advantages in comparison to other polymeric based adhesive systems, such as fast-curing rate and control of the polymerization heat evolution, being ideal for application on damaged tissues.

Herein, functionalized polymers were prepared by modifying polycaprolactone diol (PCL) with an isocyanate-functional unsaturated acrylic ester, Laromer® 9000, using two different proportions. These functionalized materials were chemically/physically characterized and, after the addition of a biocompatible photoinitiator (Irgacure® 2959), were crosslinked by UV light irradiation. Such procedure allows the obtention of flexible transparent films. Films' properties such as swelling, hydrolytic degradation, thermal stability, surface energy and adhesive capacity were evaluated. Furthermore, to assess the applicability of the films in biomedical applications, their haemocompatibility and biocompatibility were determined using human dermal fibroblasts as model.

Keywords: photocrosslinking, polyesters, bioadhesive, UV curing

1. Introduction

The production of biomaterials by photopolymerization or photocrosslinkage has shown to provide a number of advantages when compared to the heating techniques, such as: high cure rate even at room temperature, possibility of avoiding the use of certain solvents, control of polymerization temperature and elasticity, low energy requirements and high storage stability [1–4].

This procedure relies on the incidence of radiation to start the photochemical reactions in monomers, macromers or polymers, resulting in a new polymeric system. This outcome is possible due to the presence of a photoinitiator, which, by absorbing UV irradiation undergoes excitation, giving rise to free radicals, which subsequently initiate the mechanism of polymerization of the materials [5]. Herein, the efficiency of the polymerization reaction is dependent on the monomers, the photoinitiator and the beam wavelength [6]. In addition to the inherent properties of the photopolymerization technique, UV curable materials are widely used in biomedical applications, including development of drug delivery systems [7, 8], orthopaedic [9], dental restorations [10], tissue engineering [6, 11] and bioadhesives [12, 13].

The use of photopolymerization in the development of an adhesive for medical application will provide several benefits inherent to the method itself. UV curable adhesives offer major advantages such as a high cure rate, which leads to a reduction of surgical time, a reduction of trauma applied on weakened and traumatized tissues and a superior control over the final properties of the material [14–16]. Hence, a photocrosslinkable adhesive will exhibit a combination of easy application and efficacy.

The development of this type of functionalized materials was mainly registered during the second half of the 20th century. Materials such as N-vinylpyrrolidone (PVP) [17], chitosan [18], polyethylene glycol (PEG) [19], polylactic acid (PLA) [13], polycaprolactone (PCL) [12], and even polymeric blends [20], have been chemically

modified by different methods and tested as photocrosslinkable bioadhesives. Despite some promising results, such as adherence efficacy, other properties such as curing times and biocompatibility, may still be improved.

During the work reported herein, a photocrosslinkable biodegradable bioadhesive based on PCL was developed and tested as a possible surgical adhesive for treatment and regeneration of injured organic tissues. PCL is a semi-crystalline linear biodegradable aliphatic polyester with hydroxyl (OH) terminal groups, that has been used in several medical applications already approved by the US Food and Drug Administration [21]. Its structure contains several aliphatic ester linkages which may undergo hydrolysis and its degradation products can be either metabolized and naturally included in the tricarboxylic acid cycle or eliminated by renal secretion. This OH terminated polyester was functionalized with a low-viscous isocyanate-functional unsaturated acrylic ester, Laromer® LR 9000 (LAR). The produced macromer was crosslinked under UV irradiation using a biocompatible photoinitiator Ir2959 [22]. In order to evaluate its feasibility for the intended application, the synthesized materials were properly characterized. Their haemolytic and thrombogenic character were also assessed as well as their cytotoxicity in human fibroblasts culture.

2. Experimental Procedures

2.1. Materials

PCL diol (Mn ≈ 530), diethyl ether (99%), formamide (99%), diiodomethane (99%), ethylene glycol (99.8%), potassium ferrocyanide (99%), formaldehyde (37%, stabilized with methanol), nonionic surfactant Triton X®-100, Dulbecco's modified Eagle's medium (DMEM-F12), gentamicin, LB Broth, phosphate-buffered saline tablets (PBS), streptomycin and trypsin were purchased from Sigma-Aldrich (Sintra, Portugal). Laromer® LR 9000 oligomer (LAR) and photoinitiator 2-hydroxy-1-[4-(2-hydroxyethoxy)

phenyl]-2-methyl-1-propanone, under the trade name of Irgacure® 2959 (97-99%), were kindly provided by BASF (Germany) and used without purification. Potassium dihydrogen phosphate (99.5%) and calcium chloride (99.5%) were obtained from CHEM-LAB.

Anticoagulated rabbit blood (ACD blood), used in the haemocompatibility tests, was bought from PROBIOLÓGICA (Biologic Products Company; Lisbon, Portugal) and used in the same day it was received.

Normal adult human dermal fibroblasts (NHDF) were obtained from PromoCell (Labclinics, SA; Barcelona, Spain) and used in cytotoxicity experiments.

3-(4,5-dimethylthiazol-2-yl)-2,5-diphenyltetrazolium bromide (MTT) was purchased from Alfa Aesar (Ward Hill, USA). Fetal bovine serum (FBS) was purchased from Biochrom AG (Berlin, Germany).

2.2. Methods

2.2.1. Functionalization of PCL

Macromers containing urethane groups were synthesized by modification of hydroxyl end functionalized PCL with LAR using ratios of OH:NCO groups of 1:1 and 1:2. Diethyl ether was used as solvent due to its high volatility.

The reactions were performed by stirring the two components in conventional two neck round-bottomed glass flasks, in the absence of air (under a nitrogen atmosphere), and refluxing the solvent using a long condenser with a drying tube filled with calcium chloride to maintain reflux and avoid humidity.

The obtained functionalized macromers (PCL-LAR(1:1) and PCL-LAR(1:2)) exhibited a low viscosity and a transparent appearance. Finally, the materials were stored until further use.

2.2.2. UV-curing and films preparation

Ir2959 was added to each macromer in a percentage of 4% of the carbon double bonds moles, keeping the reaction glass flask in a dark environment until complete solubilisation. The final solutions were then individually poured onto Petri dishes, and then irradiated using a Multiband UV UVGL-48 model from Mineral Light® Lamp (wavelengths of 254–354 nm). Dry, transparent and flexible films were obtained after 30s for the PCL-LAR(1:1) macromer and after 60 s for PCL-LAR(1:2).

2.3. Characterization techniques

2.3.1. Attenuated Total Reflectance - Fourier Transform Infrared spectroscopy (ATR-FTIR)

ATR-FTIR analysis of the adhesives was carried out with a Jasco FT-IR-4200 spectrometer, from Jasco Inc. (Easton, USA) equipped with a Golden Gate Single Reflection Diamond ATR. Data collection was performed with 4 cm^{-1} spectral resolution and 128 accumulations.

2.3.2. Nuclear Magnetic Resonance (NMR)

The ^{1}H NMR spectra of PCL, LAR and of both prepared macromers were obtained on a 9.4 Tesla Spectrometer, at room-temperature using $CDCl_3$ as solvent. Tetramethylsilane (TMS) was used as the internal reference.

2.3.3. Water sorption capacity

Three samples of each prepared film with an area of 4 cm^2 and 1 mm thick were dried under vacuum at 60 ºC until a constant weight (W_d) was attained. The dried samples were then placed in a closed container with a saturated solution of pentahydrated copper sulphate and then they were weighted at different times until a maximum weight was achieved (W_s). Finally, water sorption (%) was assessed by using Eq. (1).

$$\text{Water sorption (\%)} = \left(\frac{W_s - W_d}{W_d}\right) \times 100 \quad (1)$$

2.3.4. Hydrolytic degradation in phosphate buffer solution (PBS)

Dried samples (n = 3) of each film (1 mm of thickness) were weighted ($W_{d,o}$), immersed in 10 mL of PBS 0.01M (pH 7.4), and then incubated for 6 weeks at 37 ºC. The films were afterwards removed from PBS, washed with distilled water and dried in vacuum conditions, at 60 ºC, until constant weight ($W_{d,t}$). The degree of degradation was calculated from the weight loss, which was determined as represented in the Eq. (2).

$$\text{Weight loss (\%)} = \frac{W_{d,0} - W_{d,t}}{W_{d,0}} \times 100 \quad (2)$$

where $W_{d,0}$ and $W_{d,t}$ are the average samples weights before the degradation test and at time *t*, respectively.

2.3.5. *In vitro* adhesion tests – Evaluation of films' adhesive capacity

In order to evaluate the bonding performance of the photocrosslinkable macromers, the formulations containing the photoinitiator were applied between gelatine sheets (dimensions 1.5 x 3 cm). The gelatine pieces containing the adhesives formulations were overlapped (active area 1.5 x 1 cm) and then irradiated under the same conditions as

described for the preparation of the films. The gelatine sheets were then subjected to the "pull to break" test at room temperature using a Chatillon TCD 1000 (Lloyd Instruments™, Ametek, USA). The assays were carried out at room temperature with a pulling velocity of 20 mm/min, and the distance between the probes was established at 1 cm. Force and length variation were recorded and tests were terminated with the fracture of the gelatine sheets or their separation until adhesion failed to occur. A plain gelatine sheet (1.5 x 5 cm) was also subjected to the same test to be used as a control.

2.3.6. Determination of surface energy by contact angle measurement

The surface energies of the films were determined, in order to compare their values with the ones obtained from literature for skin and blood. An OCA 20 unit from Dataphysics was used to measure the static contact angles at room temperature [23, 24]. All the assays were conducted on the air-facing surfaces of the films with three liquids (water, ethylene glycol formamide and diiodomethane) using the sessile drop method. Ten measurements on several points were performed on the samples surface to determine the mean static contact angle and its standard error. The surface free energies (γ_s) as well as their dispersive (γ_S^D) and polar (γ_S^P) components were assessed according to the Owens-Wendt-Rabel and Kaelble (OWRK) method [25].

2.3.7. Thermal properties

The thermal stability of PCL, LAR and the developed photocrosslinked adhesives PCL-LAR(1:1) and PCL-LAR(1:2) was evaluated in the range of ca. 25-600 ºC, in an SDT Q600 from thermal analysis, with a heating rate of 10 °C·min^{-1} under dry nitrogen purge flow of 100 mL·min^{-1}.

The glass transition temperature, T_g, was determined by DMTA with a Tritec 2000 DMA, from Triton Technology, Ltd (Keyworth, UK). The crosslinked adhesives were analysed in the single cantilever bending geometry using stainless steel material pockets. All DMTA measurements were carried out in a -150 to 200 °C temperature range, at frequencies of 1 and 10 Hz, using a heating rate of 5 °C·min^{-1}. The T_g was determined from the maximum of tan δ, at 1 Hz.

2.3.8. Haemocompatibility analysis

Blood compatibility of the UV-cured films was evaluated *in vitro* accordingly to the International Organization for Standardization (ISO) 10993-4 [26] and by assessing two types of blood interaction: thrombogenicity and haemolytic potential [27].

Surface morphology and thrombogenicity

The surface morphologies of the membranes were analysed by scanning electron microscopy (SEM). The samples were placed on double-sided graphite tape, attached onto a metal surface, and sputter-coated with gold. SEM images were acquired at 10 kV with a JSM-5310 (JEOL, Japan) scanning electron microscope.

Thrombus formation on the surface of the films (n=3) was evaluated using the gravimetric method of Imai and Nose [28]. Anticoagulated rabbit blood (ACD blood) was used for this purpose and contact time between the samples and blood was established at 40 min. The samples were previously immersed in PBS solution at 37 ºC for 24 h. Subsequently, the PBS was removed and the ACD blood (250 μL) was placed on the adhesives surface. The same amount of blood was sited over empty Petri dishes (n = 3), which acted as the positive control (100% thrombogenicity). Blood clotting tests were started with the addition of 25 μL of a 0.10 M calcium chloride solution to each sample which were posteriorly incubated at 37 ºC for 40 min. The process was terminated by adding 5 mL of distilled water to each sample. The resultant clots were fixed with 1 mL

of a 36% formaldehyde solution, dried at 37 ºC for 24 h and finally weighted. The percentage of thrombogenicity was assessed according to Eq. (3).

$$\% \text{ Thrombogenicity} = \frac{m_{\text{clot sample}} - m_{\text{average negative control}}}{m_{\text{average positive control}} - m_{\text{average negative control}}} \times 100 \quad (3)$$

Haemolytic Potential

The haemolysis tests were performed according to the American Society for Testing and Materials (ASTM) F 756-00 standard [29]. Dried samples with 21 cm^2 were placed in polypropylene test tubes and 7 mL of PBS 0.01M (pH 7.4) were added. After 24 h of incubation at 37 ºC, the PBS was removed and the samples were left to dry. Then, 7 mL of PBS and 1 mL of diluted ACD blood (10 mg/mL ± 1 mg/mL) were added to each sample (indirect contact) as well as to three samples of the same membranes with no previous incubation with PBS (direct contact). Positive and negative controls were prepared by adding the same amount of ACD blood to 7 mL of water and PBS, respectively.

The tubes were placed at 37 ºC, for 3 h, and cautiously inverted twice every 30 min for enhancing the contact between materials and blood. After incubation, the fluids were transferred to suitable tubes and centrifuged at 700-800*g*, for 15 min. The amount of haemoglobin (Hb) released by haemolysis was measured by optical densities (OD) of the supernatants at 540 nm using a spectrophotometer UV-vis (Jasco V550). The percentages of haemolysis (HI) were calculated as described in Eq. (4).

$$\% \text{ Haemolysis (HI)} = \left(\frac{OD_{\text{test}} - OD_{\text{negative control}}}{OD_{\text{positive control}} - OD_{\text{negative control}}}\right) \times 100 \quad (4)$$

2.3.9. Evaluation of films biocompatibility

Cell culture of human fibroblasts in presence of the PCL-LAR films

Cell culture in the presence of the films was performed as previously described [13, 30]. In detail, samples of each film were sterilized by ultraviolet radiation for 30 min. Then, normal human dermal fibroblasts adult (hFib) were seeded in the presence of the different films ($20x10^3$ cells/well) in 96-well plates, using DMEM-F12, supplemented with FBS (10% v/v), streptomycin (100 μg/mL) and gentamicin (100 μg/mL). Cell proliferation was monitored using an Olympus CX41 inverted light microscope (Tokyo, Japan) equipped with an Olympus SP-500 UZ digital camera.

Evaluation of cell viability in the presence of the PCL-LAR films

To characterize the cytotoxic profile of the different films, hFib ($2x10^4$ cells/well) were seeded in the presence of the materials, in 96-well plates, with 100 μL of DMEM-F12 and then incubated at 37 ºC, in a 5% CO_2 humidified atmosphere. After 24 and 72 h of incubation, an MTT assay was carried out to assess cell viability. In detail, 50 μL of MTT (5mg/mL PBS) was added to each sample followed by their incubation for 4 h, at 37 °C, in a 5% CO_2 atmosphere. After that, the medium was removed and cells were treated with 150 μL of DMSO (0.04 N) for 30 min. Subsequently, the absorbance of each well was measured at 570 nm using a microplate reader (Biorad xMark microplate spectrophotometer). Wells containing cells in the culture medium without materials were used as negative control (K-). EtOH 96% was added to wells containing cells to be used as a positive control (K+) [31]. Statistical analysis of the obtained results was performed using one-way ANOVA with the Newman-Keuls post hoc test.

2.3.10. Scanning electron microscopy analysis

Cell adhesion and proliferation at the films surface was characterized by scanning electron microscopy (SEM) analysis. Briefly, samples were washed with PBS at room temperature and fixed overnight with 2.5 % (v/v) glutaraldehyde. Then, films were frozen, freeze-dried for 3 h, and finally mounted onto aluminium stubs with double adhesive tape and sputter-coated with gold using a Quorum Q150R ES sputter coater. SEM images were acquired with an acceleration voltage of 20 kV at different magnifications in a Hitachi S-3400N Scanning Electron Microscope [13, 32].

3. Results and Discussion

3.1. Synthesis of LAR macromers

Macromers containing urethane groups were synthesized by modification of hydroxyl end functionalized PCL with the isocyanate groups, NCO of LAR. Two distinct macromers were prepared, with different molar ratios of OH:NCO groups: PCL-LAR(1:1) and PCL-LAR(1:2).

The reactions were performed by stirring the two components in a conventional two neck round-bottomed glass flasks, under a nitrogen atmosphere and refluxing the solvent using a long condenser with a drying tube filled with calcium chloride to maintain reflux and avoid humidity. The flasks were placed in a water bath at the temperature of 60 ºC. Optimal reaction time was established as 6 h. The obtained functionalized macromers PCL-LAR(1:1) and PCL-LAR(1:2) exhibited low viscosity and transparent appearance and were properly stored for further use.

Afterwards, the obtained macromers were photocrosslinked under UV irradiation using Ir2959, in a percentage of 4% of the carbon double bonds moles. Irradiation times varied with OH:NCO groups ratio and were determined to be 30 s for PCL-LAR(1:1) and 60 s

for PCL-LAR(1:2) showing that a higher amount of LAR in the composition of the macromers leads to a higher curing time. Later, the photocrosslinked macromers were physical/chemically and biologically characterized.

3.2. Chemical characterization

ATR-FTIR and ^{1}H NMR techniques were used to follow the reactions and to prove the success of the macromers synthesis. The ATR-FTIR spectra of the developed adhesives as well of the components of the formulations are presented in Fig.1. The CH_2 stretching region, at 2800 cm^{-1} was detected as well as the typical isocyanate band, around 2260 cm^{-1}, characteristic of LAR [13]. The presence of this band on the spectrum of the final adhesives suggest that there are free NCO groups [33]. These NCO free groups present on the adhesives structure are crucial, since they will enhance the adhesion capacity to the substrate surface. The N-H stretching band was also detected, at 3360 cm^{-1} and at 1650-1550 cm^{-1} in LAR and adhesives spectra [34]. The ester group was detected in all the spectra, around 1730 cm^{-1}. The presence of the carbon double bonds (C=C) was confirmed with a band at 1680 cm^{-1}.

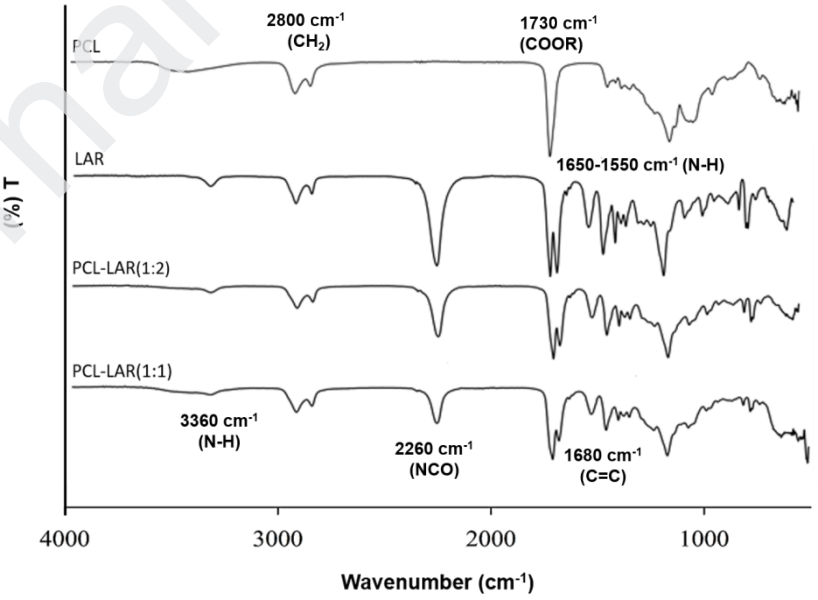

Fig.1. ATR-FTIR of PCL, LAR and the developed macromers.

Fig.2 shows the obtained ^{1}H NMR spectra of (1) PCL, (2) LAR and both macromers prepared: (3) PCL-LAR(1:1) and (4) PCL-LAR(1:2). In the PCL spectrum the typical backbone peaks are observed at (a) 1.4 ppm, (b) 1.7 ppm, (c) 2.4 ppm and (f) 4.0 ppm assigned to -C(O)OCH2CH2CH2-, -C(O)OCH2CH2CH2CH2CH2-, -CH2C(O)O- and -C(O)OCH2CH2, respectively, as well as the methylene protons of the molecular chain terminal (-CH2OH) at (d) 3.6 ppm [35, 36]. All these peaks can be seen in both macromer spectra with the exception of the later one, which confirms the linkage of the PCL terminal OH groups with the NCO groups of LAR [13], leading to the appearance of a new peak (o) at around 3.1 ppm, which was assigned to the urethane groups ($-NHCH_2-$) [13, 20, 36]. Moreover, the vinylic protons of LAR from 5.9 to 6.5 ppm (h) are also present in the macromers spectra, confirming the success of the reaction.

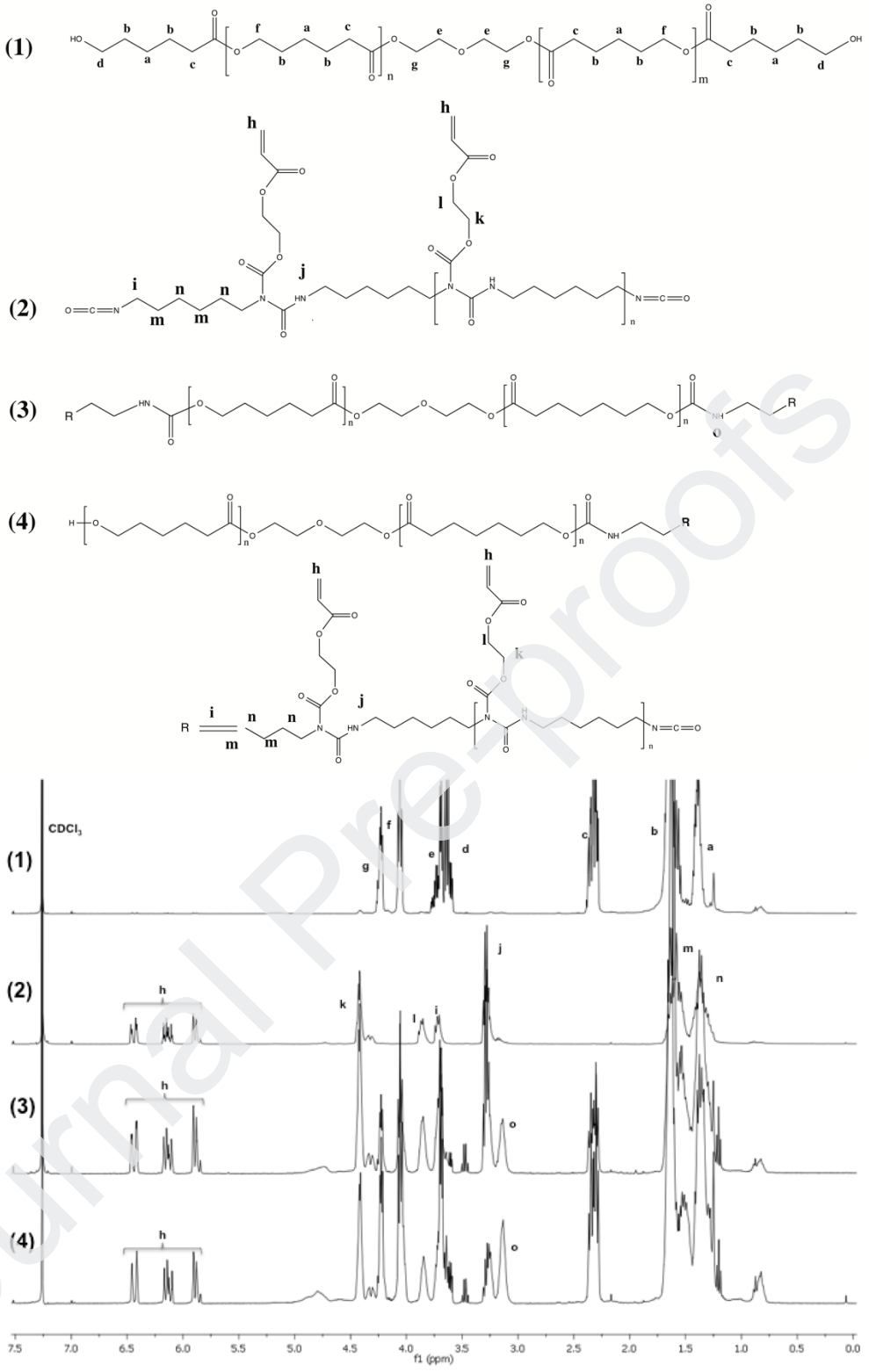

Fig.2. ^{1}H NMR spectra of PCL, LAR and the macromers PCL-LAR (1:1) and PCL-LAR(1:2). The numbered signals correspond to the protons assigned to the displayed structure.

3.3. Water sorption capacity

Adhesives volume increase (swelling) caused by water sorption is an important characteristic to evaluate the suitability of the materials for tissue engineering applications. Surgical adhesives designed for wound closure must help in the healing process and promote the healing of the damaged tissue [12, 13]. A certain percentage of swelling is benefic to facilitate the tissue regeneration; above 20%, the volume increase is too high and prejudicial for the healing process to occur, since it is responsible for causing inflammatory responses, compression of the vascular structures of the surrounding tissues, and keeping the wound limits apart [12, 13].

Materials swelling degree was evaluated after 6 weeks of incubation in a water saturated atmosphere, using three samples of each film. The results presented in Fig.3 show that, although the materials present similar swelling values, a higher amount of LAR, increases water sorption capacity, as it can be seen in functionalized PCL samples PCL-LAR(1:1) (5.8 ± 0.1%) and PCL-LAR(1:2) (7.0 ± 0.7%).

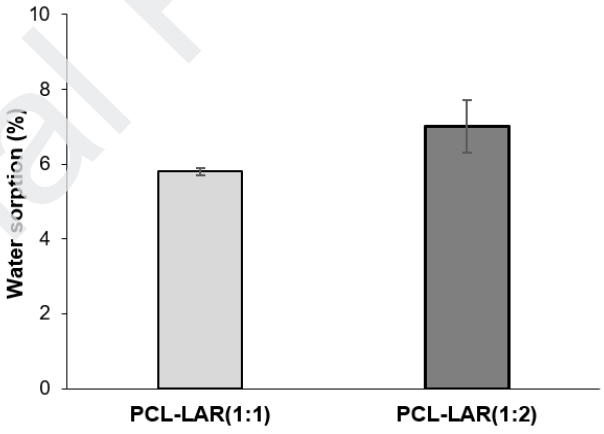

Fig.3. Water sorption of the crosslinked films after 6 weeks of incubation.

All the analysed samples proved to be suitable to be applied as wound dressings since they exhibit moderated swelling degrees that fit the requirements and the hydrophilic nature of the final adhesives contributes to improve their biocompatibility.

3.4. Hydrolytic degradation in phosphate buffer solution (PBS)

Tissue adhesives must be easy to remove, or degradable *in vivo* to biologically compatible components or in products that can be excreted by the body. The analysis of materials degradation when placed in an environment similar to the medium in which they will be applied, is fundamental to understand their biodegradability and decide about their final application [13, 37, 38].

The weight loss evaluation was performed by incubating the synthesized materials in PBS at 37 ºC. Fig.4 presents the weight loss percentage after 6 weeks incubation in the buffer solution and it shows that the material with higher proportion of LAR exhibits similar hydrolytic degradation (0.5 ± 0.078%) when compared with PCL-LAR(1:1) (0.7 ± 0.1%). These results are consistent with the reported swelling degrees and show that LAR amount do not influences significantly the weight loss percentage of the final material. Also, due to the slow degradation rates, these materials are suitable to external applications, as is the case for cyanoacrylates adhesives [13].

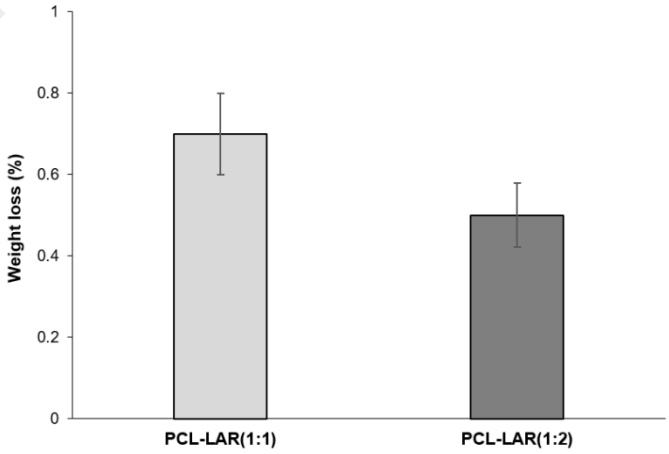

Fig.4 Hydrolytic degradation (% of weight loss) of the prepared materials in PBS.

3.5. *In vitro* adhesion tests – Evaluation of the adhesive capacity

One important property required for adhesives is the ability to adhere to living tissues, in order to assist the healing process. To evaluate this capacity, the maximum rupture force (N) was determined by performing mechanical tensile tests. The different materials were applied between two gelatine sheets, since this substrate mimics the presence of amino groups in the living tissues [13, 39]. Each assay ended by doing the "pull to break" test to analyse if the gelatine sheets fracture or separate. All the materials presented satisfactory adhesion results since gelatine sheets ruptured. According with Fig.5, the sample prepared with PCL-LAR(1:2) exhibited maximum force of 97.5 ± 5.6N, which is higher than the substrate alone (89.2 ± 3.7). Comparing with PCL-LAR(1:1) sample (70 ± 2.8N), it was found that a higher amount of LAR improves the adhesion capacity of the material. The free isocyanate groups of the adhesive structure react with the amino groups of the gelatine, forming urea linkages and promoting a greater adhesion [39]. These results are consistent with the FTIR spectra, which show the presence of peaks related to the isocyanate groups of the final materials PCL-LAR(1:1) and PCL-LAR(1:2).

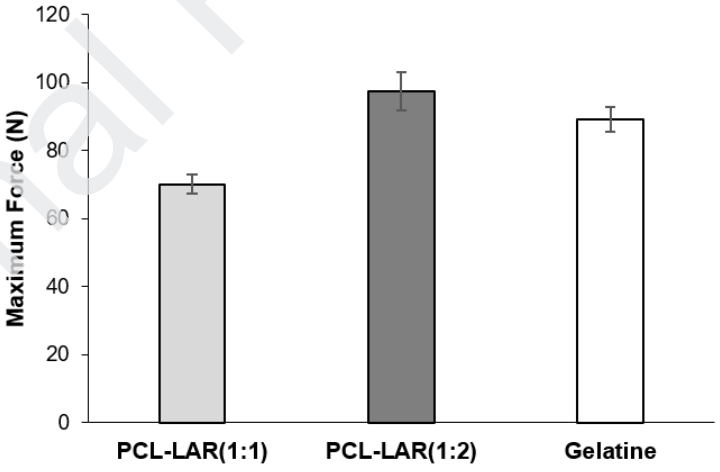

Fig.5. Values of maximum force registered during "pull to break" for gelatin sheet (control) and gelatin sheets glued with each macromer.

3.6. Determination of surface energy by contact angle measurement

In order to determine the surface energy of the developed adhesives, the contact angles were determined using specific liquids. Therefore, the surface energy of the macromers was calculated from the contact angle values, using the Owens and Wendt equation and the obtained values are given in Tab.1. The surface energy of gelatine sheet was also determined, for comparison purposes, alongside with skin [40] and blood [41, 42] literature values.

According to Tab.1, the γ_s of the macromers are lower than those obtained for the gelatine sheet, skin and blood which is a good indicator of the viability of the synthesized material as adhesives. These is one of the main requirements to ensure the adhesion to a substrate, since the surface energy of the adhesive must be equal to or less than that of the adherent [40]. Also, based on the ratio between polar and dispersive parts it is possible to predict the adhesion behaviour of the macromers. Concerning the adhesive PCL-LAR(1:1), the polar and dispersive components are very similar, therefore more interactions between the phases and a higher adhesion is to be expected. For PCL-LAR(1:2), the polar component is higher than the dispersive component which is explained by the higher amount of the urethane linkages, which ultimately lead to an increase on the polar interactions by hydrogen bonds formation [43].

Table 1. Surface energies/superficial tensions (mN/m) and their dispersive (γ_S^D) and polar (γ_S^P) components.

Substrate	Surface energies and surface tensions (mN/m)		
	γ_S	γ_S^D	γ_S^P
Gelatine	44.1 ± 2.3	5.3 ± 0.6	38.9 ± 2.2
Skin	43.7	35.7	8.0
Blood	47.5	11.2	36.3
PCL-LAR(1:1)	30.4 ± 2.2	15.4 ± 1.0	15.0 ± 1.2
PCL-LAR(1:2)	34.9 ± 2.0	9.7 ± 0.8	25.2 ± 1.8

3.7. Thermal properties

The thermal stability of the photocrosslinked macromers was assessed by TGA and the thermogravimetric curves and respective derivatives are displayed in Fig.6. The temperatures of maximum degradation were determined considering the derivative curves and the results are shown in Tab.2. According to Fig.6 the adhesives exhibit a good thermal stability, showing the first decomposition at 250 ºC, ascribed to the degradation of the urethane bonds [13].

A second and a third decomposition step was observed, for both adhesives, around 350 ºC and 460 °C, respectively. This second major degradation step can be assigned to the degradation of the ester bonds present in the soft segment of the urethane [44] and it is slightly higher than the PCL, due to an increase at the hard segments, by the formation of hydrogen bonds between NH and CO groups [33]. Although the T_d obtained for the adhesives is quite similar, PCL-LAR(1:2) shows a slightly higher T_d, which can be explained by the higher amount of LAR in the adhesive structure. Finally, the third decomposition step, detected at 456.42 ºC and 463.47 ºC for PCL-LAR(1:1) and PCL-LAR(1:2), respectively, is attributed to the decomposition of bonds of higher energy such

as C=O, C=C, C–O and C–H bonds. Overall and regarding the intended application, the adhesives showed to be stable at physiological temperature (37 ºC).

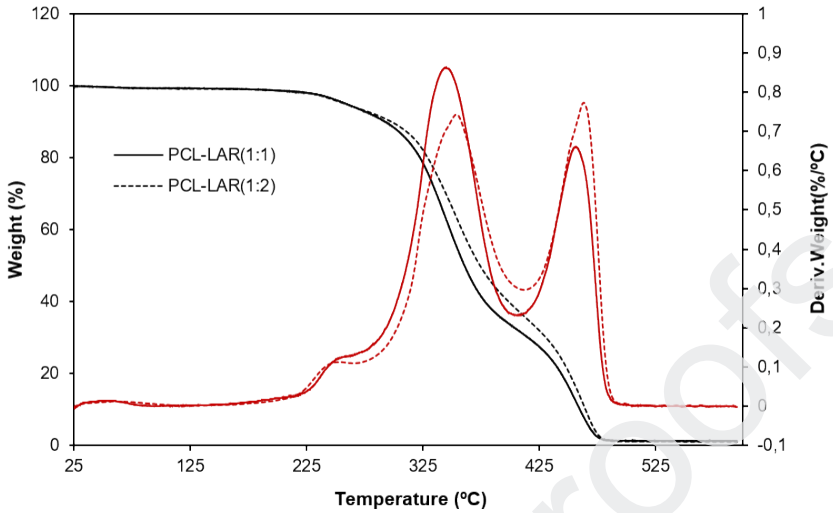

Fig.6. TGA thermograms and derivate thermogravimetric curves of PCL-LAR(1:1) and PCL-LAR(1:2).

The glass transition temperature, T_g, of the prepared adhesives was determined by dynamic mechanical thermal analysis (DMTA). DMTA is a highly sensitive technique that allows the detection of all the relaxation temperatures. During the assays, the storage modulus (elastic response, E′) and loss modulus (viscous response, E″) of each sample, under oscillating load, are monitored against time, temperature, or frequency of oscillation. Their ratio (E″/E′) defines the loss tangent (tan δ) [45]. The obtained results are presented in Tab.2 and Fig.7.

The T_g of PCL-LAR(1:1) and PCL-LAR(1:2) obtained at 1Hz, appeared at -86.31 ºC and -75.13 ºC, respectively. The adhesives exhibit a single T_g, indicating miscibility of the components of the adhesives. Also, T_g increased with the increase of the NCO proportion, which is expectable since a higher OH:NCO ratio led to a more crosslinked

material, due to the formation of more urethane linkages, thus a higher amount of energy is necessary to promote chain mobility.

Table 2. Thermal properties of the developed adhesives, T_d (onset of decomposition temperature) and T_g (glass transition temperature), determined by DMTA.

Sample	$T_{5\%}$ (ºC)	$T_{10\%}$ (ºC)	T_{dmax}			T_g (ºC)
			1st stage (ºC)	2nd stage (ºC)	3rd stage (ºC)	
PCL	195.82	219.34	243.81	319.6	-	-
LAR	225.86	240.64	245.19	326.21	466.09	-
PCL-LAR(1:1)	257.53	292.16	251.51	346.30	456.42	-86.31
PCL-LAR(1:2)	256.57	297.59	248.10	353.92	463.47	-75.13

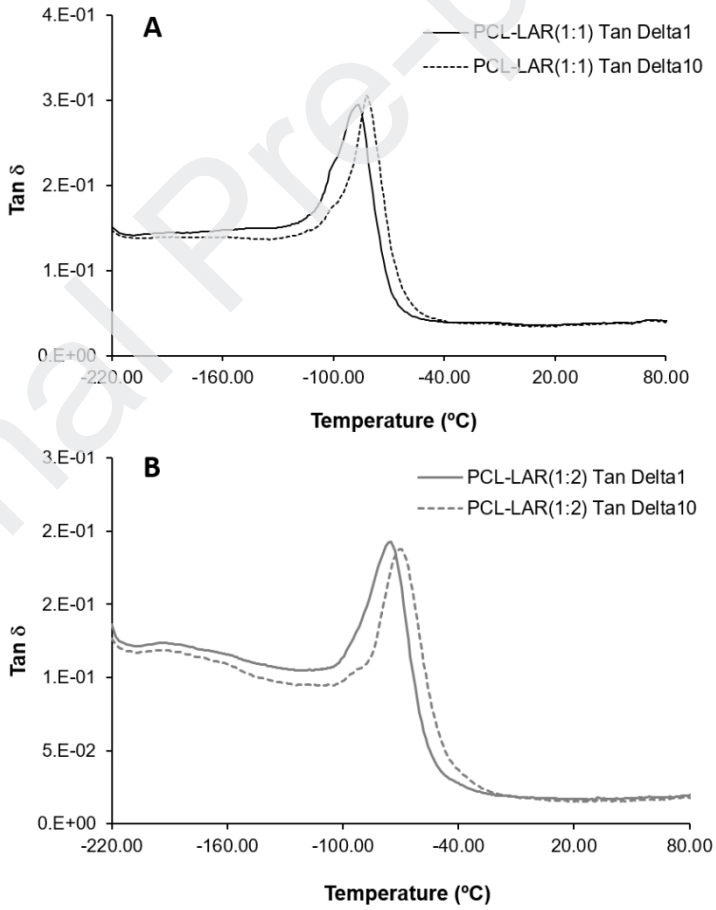

Fig.7. DMTA thermograms of the macromers, at frequencies of 1 and 10 Hz, under a heating rate of 5 °C·min^{-1}.

3.8. Haemocompatibility assessment

3.8.1. Surface morphology and thrombogenicity

Thrombogenicity is related with the ability of a surface to induce blood clotting and therefore the creation of thrombus. This phenomenon has been associated with several surfaces' characteristics such as surface energy, charge and surface roughness [46, 47]. During this work, the surface of the photocrosslinked membranes was observed by SEM (Fig.8) and no morphological differences were observed between the samples. Also, both surfaces proved to be quite regular and with no significant roughness.

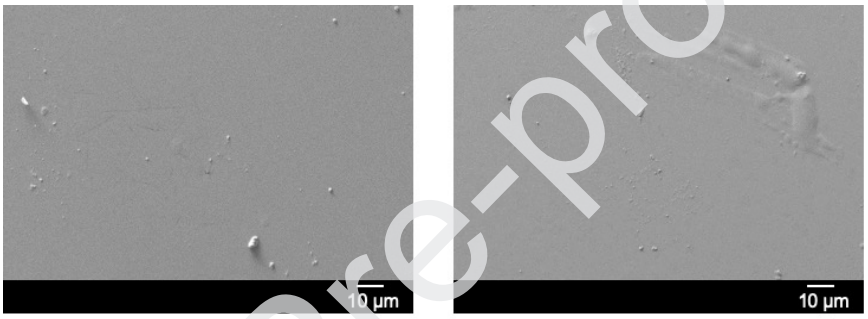

Fig.8. SEM images of the surface morphology of the (A) PCL-LAR(1:1) and (B) PCL-LAR(1:2) at a magnification of 500x.

However, and despite the smoothness of the surfaces, high values of thrombogenicity were registered for both samples (Fig.9) meaning that roughness was not the key factor influencing clotting in these materials. Other authors have reported similar results when assessing thrombogenicity and concluded that the inherent chemical characteristics of the surface, such as wettability and interfacial free energy played a more significant role in the thrombosis mechanism than the surface's morphology [48].

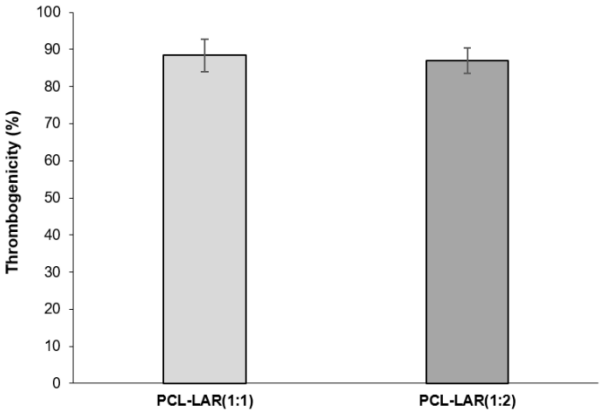

Fig.9. Thrombogenicity (%) of the crosslinked materials after 45 min of contact with blood.

Several studies have shown that thrombogenicity is directly related to the value of energy presented by a surface [49]. More specifically, low surface energy values are reported to be an important factor on the first stage of the coagulation cascade that ends in thrombus formation [50]. Considering the materials herein produced, it was verified that both presented low surface energy levels and are in fact thrombogenic. This type of surfaces presents an increased ability of adsorbing plasma proteins when comparing with hydrophilic ones. While in hydrophilic surfaces the water molecules are strongly bounded hampering protein adsorption, in hydrophobic surfaces water molecules are easily displaced by plasma proteins which, once adsorbed, trigger the complex series of events leading to thrombosis [51].

3.8.2. Haemolytic potential

Haemolysis is described as the breakdown of erythrocytes with subsequent release of intracellular contents [52]. The disruption of the erythrocytes' membranes increases levels of free plasma haemoglobin capable of inducing toxic effects or other effects which may stress the kidneys or other organs and is therefore an undesirable effect for any material designed to be applied *in vivo* [29]. The haemolysis index of the prepared

membranes was evaluated according to ASTM F 756-00 [29] using the cyanmethaemoglobin method which allows quantifying levels of plasma haemoglobin that may not be measurable under in vivo conditions. The haemolysis results obtained for all samples during direct and indirect contact with blood showed that both materials are classified as non-haemolytic (haemolytic index <2) (Fig.10).

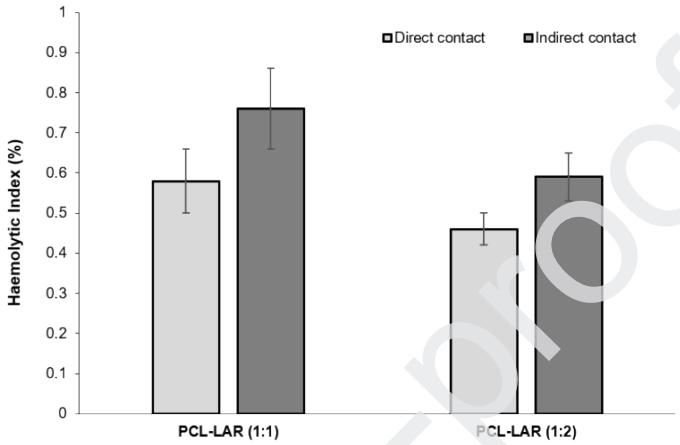

Fig.10. Values of haemolysis (%) of PCL-LAR(1:1) and PCL-LAR(1:2).

These results indicate that no disruption of the erythrocyte membranes and consequent Hb release is verified during incubation in the anticoagulated blood during HI assessment. For this reason, materials are considered blood-compatible which is a fundamental feature considering the intended biomedical application.

3.9. Evaluation of films biocompatibility

The cytotoxic profile of the produced films was evaluated through an MTT assay. A model cell line of hFib was seeded over the film samples. As can be observed, for both film samples, cells were able to adhere and proliferate during 72 h (Fig.11A). During this period, no acute cytotoxic effect was registered, suggesting that these films may be promising candidates for the intended application (Fig.11B). Additionally, SEM images

of hFib in contact with the films were also acquired, where it is possible to verify that cells were able to adhere and spread at the surface of the different samples along 72 h of incubation (Fig.11C). Such features are crucial for improving the healing process.

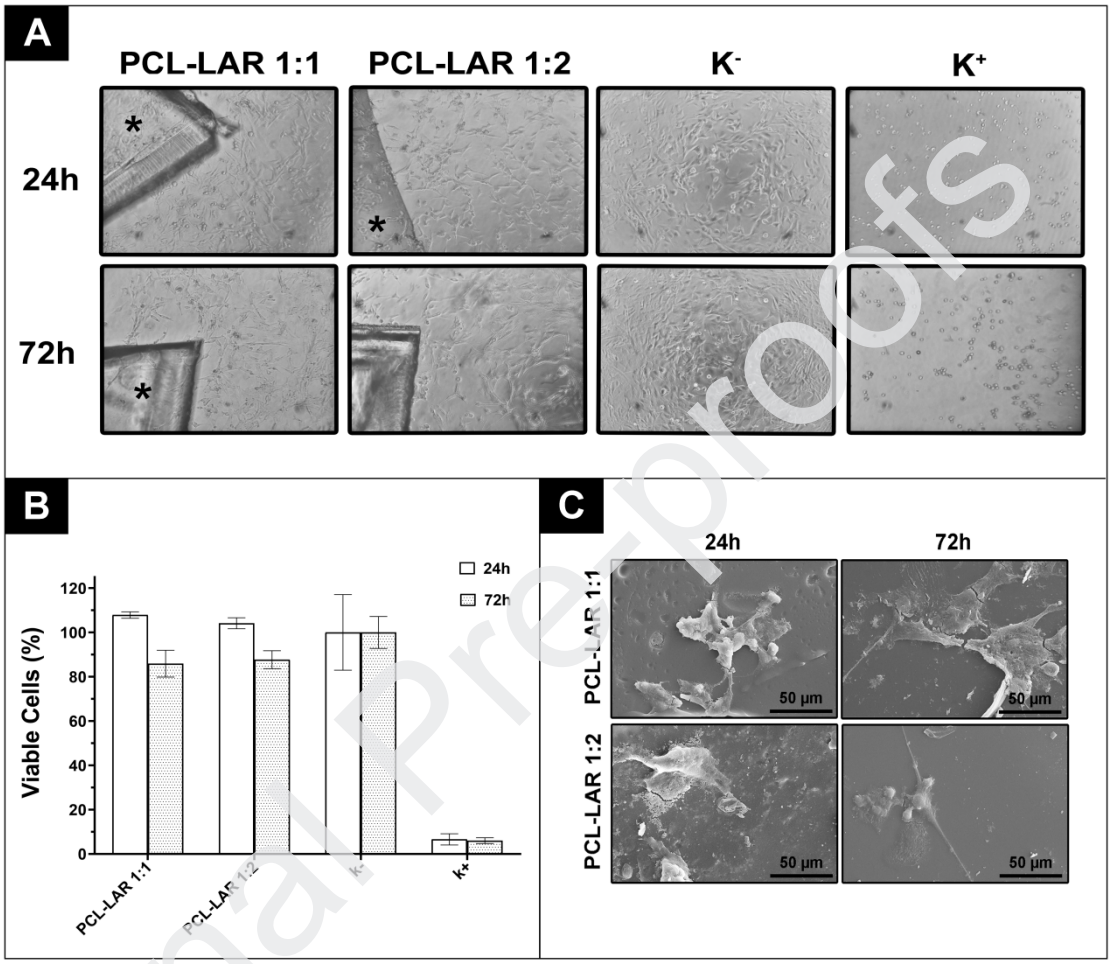

Fig.11. **A**. Microscopic images of hFib in contact with the different films after 24 and 72h of incubation at a magnification of 100×; **B**. Characterization of the hFib viability in contact with the different films after 24 and 72 h; live cells (K-); dead cells (K+). Each result represents the mean ± standard deviation of the mean of at least three independent experiments. Statistical analysis was performed using one-way ANOVA with Newman-Keuls post hoc test (*$p<0.05$); **C**. SEM images of hFib adhesion and elongation at the surface of the different films after 24 and 72 h of incubation.

4. Conclusions

PCL was chemically modified with two different proportions of LAR in order to incorporate carbon-carbon double bounds while maintaining free isocyanate groups in the final macromer structure. These chemical modifications were confirmed by ATR-FTIR and by ^{1}H NMR analyses. The adhesion capacity tests of the developed macromers using gelatine sheets as the substrate demonstrated that they were able to promote adhesion and that the breaking point was similar to the gelatine maximum force. Also, the adhesive capacity was improved when LAR proportion was increased due to the existence of NCO free groups.

Crosslinked films were then prepared by UV irradiation of these macromers and by using Ir2959 as the photoinitiator, yielding flexible crosslinked networks after 30 and 60 s. These films were characterized in terms of swelling capacity and hydrolytic degradation. The samples presented a low water sorption capacity as well as slow degradation rates and therefore more suitable to external application. While thermal degradation profiles were quite similar for both chemical compositions, T_g was shown to increase with a higher amount of LAR in the polymeric structure due to a more effective crosslinking process.

Concerning haemocompatibility, both materials showed to be thrombogenic due to their low surface energy values. In addition, the haemolytic indexes showed to be lower than 2 and therefore these materials are classified as non-haemolytic.

In vitro studies showed that, despite all materials presenting a biocompatible profile after 24 h, a higher amount of LAR, and therefore a higher crosslinking degree, had a positive impact on the biocompatibility of the materials after 72 h of cells being in contact with them.

Based on the overall results, PCL-based macromers present suitable characteristics and are good candidates to be used in the near future as surgical adhesives.

5. Acknowledgement

This work was supported by the Portuguese Foundation for Science and Technology thought the project FCT Researcher IF/01432/2015.

Data availability

The raw/processed data required to reproduce these findings cannot be shared at this time due to technical or time limitations.

References

[1] P. Ferreira, J. F. J. Coelho, J. F. Almeida, and M. H. Gil, "Photocrosslinkable Polymers for Biomedical Applications," *Biomed. Eng. - Front. Challenges*, pp. 55–74, 2009.

[2] J. Seppälä, H. Korhonen, R. Hakala, and M. Malin, "Photocrosslinkable polyesters and poly(ester anhydride)s for biomedical applications," *Macromol. Biosci.*, vol. 11, no. 12, pp. 1647–1652, 2011.

[3] D. S. Marques *et al.*, "Photocurable bioadhesive based on lactic acid," *Mater. Sci. Eng. C*, vol. 58, no. January, pp. 601–609, 2016.

[4] J. H. Moon, Y. G. Shul, S. Y. Hong, Y. S. Choi, and H. T. Kim, "A study on UV-curable adhesives for optical pick-up: I. Photo-iniciator effects," *Int. J. Adhes. Adhes.*, vol. 25, no. 6, pp. 534–542, 2005.

[5] D. Christian, "Kinetic Study and New Applications of UV Radiation Curing," *Macromol. Rapid Commun.*, vol. 23, no. 18, pp. 1067–1093, 2003.

[6] J. L. Ifkovits and J. A. Burdick, "Review: Photopolymerizable and Degradable

Biomaterials for Tissue Engineering Applications," *Tissue Eng.*, vol. 13, no. 10, pp. 2369–2385, 2007.

[7] S. Lu and K. S. Anseth, "Photopolymerization of multilaminated poly (HEMA) hydrogels for controlled release," *J. Control. Release*, vol. 57, pp. 291–300, 1999.

[8] J. F. Almeida, P. Ferreira, A. Lopes, and M. H. Gil, "Photocrosslinkable biodegradable responsive hydrogels as drug delivery systems," *Int. J. Biol. Macromol.*, vol. 49, no. 5, pp. 948–954, 2011.

[9] D. S. Muggli, A. K. Burkoth, and K. S. Anseth, "Crosslinked polyanhydrides for use in orthopedic applications: Degradation behavior and mechanics," *J. Biomed. Mater. Res.*, vol. 46, no. 2, pp. 271–278, 1999.

[10] A. Gatti, A. N. S. Rastelli, S. J. L. Ribeiro, Y. Messaddeq, and V. S. Bagnato, "Polymerization of photocurable commercial dental methacrylate-based composites : Photocalorimetry study," *J. Therm. Anal. Calorim.*, vol. 87, no. 3, pp. 631–634, 2007.

[11] K. T. Nguyen and J. L. West, "Photopolymerizable hydrogels for tissue engineering applications," *Biomaterials*, vol. 23, no. January, pp. 4307–4314, 2002.

[12] P. Ferreira, J. F. J. Coelho, and M. H. Gil, "Development of a new photocrosslinkable biodegradable bioadhesive," *Int. J. Pharm.*, vol. 352, no. 1–2, pp. 172–181, 2008.

[13] J. M. C. Santos *et al.*, "Synthesis, functionalization and characterization of UV-curable lactic acid based oligomers to be used as surgical adhesives," *React. Funct. Polym.*, vol. 94, 2015.

[14] R. S. Benson, “Use of radiation in biomaterials science,” *Nucl. Instruments Methods Phys. Res. B*, vol. 191, no. 1–4, pp. 752–757, 2002.

[15] M. Mehdizadeh and J. Yang, “Design Strategies and Applications of Tissue Bioadhesives,” *Macromol. Biosci.*, vol. 13, no. 3, pp. 271–288, 2013.

[16] A. P. Duarte, J. F. Coelho, J. C. Bordado, M. T. Cidade, and M. H. Gil, “Surgical adhesives: Systematic review of the main types and development forecast,” *Prog. Polym. Sci.*, vol. 37, no. 8, pp. 1031–1050, 2012.

[17] F. J. Kao, G. Manivannan, and S. P. Sawan, “UV curable bioadhesives: Copolymers of N-vinyl pyrrolidone,” *J. Biomed. Mater. Res.*, vol. 38, no. 3, pp. 191–196, 1997.

[18] K. Ono *et al.*, “Experimental evaluation of photocrosslinkable chitosan as a biologic adhesive with surgical applications,” *Surgery*, vol. 130, no. 5, pp. 844–850, 2001.

[19] M. W. Grinstaff, “Designing hydrogel adhesives for corneal wound repair,” *Biomaterials*, vol. 28, no. 35, pp. 5205–5214, 2007.

[20] T. M. Cernadas *et al.*, “sPreparation of biodegradable functionalized polyesters aimed to be used as surgical adhesives,” *Eur. Polym. J.*, vol. 117, no. May, pp. 442–454, 2019.

[21] B. Azimi, P. Nourpanah, M. Rabiee, and S. Arbab, “Poly (ε -caprolactone) Fiber: An Overview,” *J. Eng. Fiber. Fabr.*, vol. 9, no. 3, pp. 74–90, 2014.

[22] C. G. Williams, A. N. Malik, T. K. Kim, P. N. Manson, and J. H. Elisseeff, “Variable cytocompatibility of six cell lines with photoinitiators used for polymerizing hydrogels and cell encapsulation,” *Biomaterials*, vol. 26, no. 11, pp. 1211–1218, 2005.

[23] Y. Yuan and T. R. Lee, “Contact Angle and Wetting Properties,” in *Surface Sciences*, Springer S., vol. 51, G. Bracco and B. Holst, Eds. Heidelberg, Berlin: Springer, 2013, pp. 3–34.

[24] F. Hejda, P. Solar, and J. Kousal, “Surface Free Energy Determination by Contact Angle Measurements – A Comparison of Various Approaches,” *WDS’10 Proc. Contrib. Pap.*, vol. 52, no. 5, pp. 1457–1461, 2010.

[25] A. Rudawska, “Adhesive Properties,” in *Scanning Electron Microscopy*, V. Kazmiruk, Ed. IntechOpen, 2012, pp. 101–126.

[26] “ISO 10993-4:2002, Biological evaluation of medical devices. Part 4: Selection of tests for interactions with blood,” 1999.

[27] P. Alves, R. Cardoso, T. R. Correia, B. P. Antunes, I. J. Correia, and P. Ferreira, “Surface modification of polyurethane films by plasma and ultraviolet light to improve haemocompatibility for artificial heart valves,” *Colloids Surfaces B Biointerfaces*, vol. 113, 2014.

[28] Y. Imai and Y. Nose, “A new method for evalution of antithrombogenicity of materials,” *J. Biomed. Mater. Res.*, vol. 6, no. 3, pp. 165–172, 1972.

[29] “ASTM F756-00, Standard Practice for Assessment of Hemolytic Properties of Materials,” 2000.

[30] M. P. Ribeiro *et al.*, “Development of a new chitosan hydrogel for wound dressing,” *Wound Repair Regen.*, vol. 17, no. 6, pp. 817–824, 2009.

[31] T. R. Correia *et al.*, “3D Printed scaffolds with bactericidal activity aimed for bone tissue regeneration,” *Int. J. Biol. Macromol.*, vol. 93, pp. 1432–1445, 2016.

[32] P. H. Castilho *et al.*, “Modification of microfiltration membranes by hydrogel impregnation for pDNA purification,” *J. Appl. Polym. Sci.*, vol. 132, no. 21, p.

41610, 2015.

[33] M. F. Valero and Y. Ortegón, “Polyurethane elastomers-based modified castor oil and poly(ε-caprolactone) for surface-coating applications: Synthesis, characterization, and in vitro degradation,” *J. Elastomers Plast.*, vol. 47, no. 4, pp. 360–369, 2015.

[34] J. Coates, “Interpretation of Infrared Spectra , A Practical Approach Interpretation of Infrared Spectra , A Practical Approach,” *Encyclopedia of Analytical Chemistry*. John Wiley& Sons Ltd, Chichester, pp. 10815–10837, 2000.

[35] K. Żółtowska, M. Sobczak, and E. Oledzka, “Novel zinc catalytic systems for ring-opening polymerization of ε-caprolactone,” *Molecules*, vol. 20, no. 2, pp. 2816–2827, 2015.

[36] S.-Y. Lee *et al.*, “Synthesis and Characterization of Polycaprolactone-Based Polyurethanes for the Fabrication of Elastic Guided Bone Regeneration Membrane,” *Biomed Res. Int.*, vol. 2018, pp. 1–13, 2018.

[37] P. Ferreira, M. H. Gil, and P. Alves, *An overview in surgical adhesives*. 2013.

[38] H. K. Makadia and S. J. Siegel, “Poly Lactic-co-Glycolic Acid (PLGA) as Biodegradable Controlled Drug Delivery Carrier,” *Polymers (Basel).*, vol. 3, pp. 1377–1397, 2011.

[39] P. Ferreira, A. F. M. Silva, M. I. Pinto, and M. H. Gil, “Development of a biodegradable bioadhesive containing urethane groups,” *J. Mater. Sci. Mater. Med.*, vol. 19, no. 1, pp. 111–120, 2008.

[40] S. Venkatraman and R. Gale, “Skin adhesives and skin adhesion. 1. Transdermal drug delivery systems,” *Biomaterials*, vol. 19, no. 13, pp. 1119–1136, 1998.

[41] S. Agathopoulos and P. Nikolopoulos, “Wettability and interfacial interactions in bioceramic-body-liquid systems,” *J. Biomed. Mater. Res.*, vol. 29, no. 4, pp. 421–429, 1995.

[42] J. Y. Chen *et al.*, “Antithrombogenic investigation of surface energy and optical bandgap and hemocompatibility mechanism of Ti(Ta+5)O2 thin films,” *Biomaterials*, vol. 23, no. 12, pp. 2545–2552, 2002.

[43] P. Król and B. Król, “Surface free energy of polyurethane coatings with improved hydrophobicity,” *Colloid Polym. Sci.*, vol. 290, no. 10, pp. 879–893, 2012.

[44] M. Malik and R. Kaur, “Mechanical and Thermal Properties of Castor Oil–Based Polyurethane Adhesive: Effect of TiO2 Filler,” *Adv. Polym. Technol.*, vol. 37, no. 1, pp. 24–30, 2018.

[45] P. Ferreira, J. Coelho, K. Dos Santos, E. Ferreira, and M. Gil, “Thermal characterization of chitosan-grafted membranes to be used as wound dressings,” *J. Carbohydr. Chem.*, vol. 25, no. 2–3, pp. 233–251, 2006.

[46] P. Mulinti, J. E. Brooks, B. Lervick, J. E. Pullan, and A. E. Brooks, *Strategies to improve the hemocompatibility of biodegradable biomaterials*. Elsevier Ltd., 2017.

[47] P. Ferreira, P. Alves, P. Coimbra, and M. H. Gil, “Improving polymeric surfaces for biomedical applications: a review,” *J. Coatings Technol. Res.*, vol. 12, no. 3, 2015.

[48] T. Hasebe *et al.*, “Effects of surface roughness on anti-thrombogenicity of diamond-like carbon films,” *Diam. Relat. Mater.*, vol. 16, no. 4–7, pp. 1343–1348, 2007.

[49] C. Zhao, X. Liu, M. Nomizu, and N. Nishi, “Blood compatible aspects of DNA-

modified polysulfone membrane - Protein adsorption and platelet adhesion," *Biomaterials*, vol. 24, no. 21, pp. 3747–3755, 2003.

[50] L. Poussard *et al.*, "In vitro thrombogenicity investigation of new water-dispersible polyurethane anionomers bearing carboxylate groups," *J. Biomater. Sci. Polym. Ed.*, vol. 16, no. 3, pp. 335–351, 2005.

[51] L.-C. Xu, J. Bauer, and C. A. Siedlecki, "Proteins, Platelets, and Blood Coagulation at Biomaterial Interfaces," *Colloids Surf B Biointerfaces*, vol. 124, pp. 49–68, 2014.

[52] A. K. Saenger and N. Korpi-Steiner, "Advances in Cardiac Biomarkers of Acute Coronary Syndrome," *Adv. Clin. Chem.*, vol. 78, pp. 1–58, 2017.

Graphical abstract

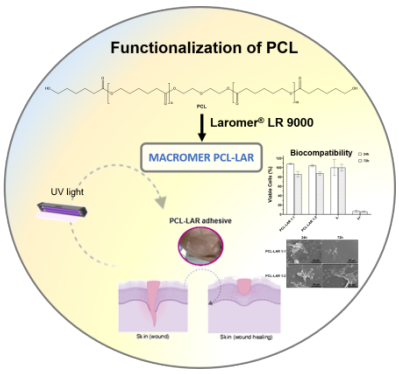

Highlights

- Photocrosslinkable PCL based macromers were synthesized by functionalization with Laromer® 9000;
- The macromers were crosslinked via UV irradiation using Irgacure 2959® as the photoinitiator;
- All samples showed to be thrombogenic and non-haemolytic;
- Higher crosslinking degrees had a positive impact on the biocompatibility.